Presentation of Ileal Burkitt Lymphoma in Children

Joseph R. Grajo[1*], Mark L. Kayton[2], Thora S. Steffensen[3], Natasa Dragicevic[1], Claude B. Guidi[1]

1. Department of Radiology, University of South Florida, Tampa, Florida, USA

2. Division of Pediatric Surgery, Department of Surgery, University of South Florida, Tampa, Florida, USA

3. Department of Pathology, Tampa General Hospital, Tampa, Florida, USA

* **Correspondence:** Joseph R. Grajo, M.D., Department of Radiology, University of South Florida, 12901 Bruce B Downs Blvd, Box 17, Tampa, FL 33612, USA
(*jgrajo@health.usf.edu*)

Radiology Case. 2012 Aug; 6(8):27-38 :: DOI: 10.3941/jrcr.v6i8.1052

ABSTRACT

Burkitt lymphoma is a highly aggressive form of Non-Hodgkin lymphoma that responds favorably if diagnosed accurately and treated early. Recognition of the various radiologic manifestations of Burkitt lymphoma can help guide the clinician to expedite appropriate chemotherapy. We present two cases that illustrate different radiologic presentations of this aggressive gastrointestinal malignancy in children. Case 1 features a 7-year-old boy who presented to our hospital with recurrent ileocecal intussusception. Case 2 describes a 16-year-old male with history of blood-streaked stools. Ileocectomy was performed in both cases and histologic analysis showed the "starry sky pattern" and t(8;14) translocation, classic for Burkitt lymphoma. Both patients remain disease-free following surgical excision and chemotherapy.

CASE REPORT

CASE REPORT

Case 1

A 7 year-old previously healthy Caucasian boy presented with a one week history of abdominal pain, two day history of constipation, and one day history of nausea and vomiting. Focused abdominal sonography was performed using a GE M12L transducer with pediatric abdomen settings at 9 MHz frequency. This demonstrated a reniform-appearing mass and free fluid in the right lower quadrant, suspicious for intussusception [Fig. 1]. Subsequently, computed tomography (CT) of the abdomen/pelvis with intravenous and rectal contrast was obtained utilizing a Phillips Brilliance 64 slice CT scanner at 78 mA and 80 kV with 3 mm slice thickness. CT confirmed suspicion of ileocecal intussusception [Fig. 2]. Therefore, an air contrast enema was ordered to attempt nonsurgical reduction. The patient was taken to the fluoroscopy suite, where a soft tip catheter was placed intra-rectally and taped into position. Using fluoroscopic guidance, a sphygmometer was used with 120 mmHg pop off for maximum air pressure. Air was pumped into the colon for 5 minutes. Real time fluoroscopy demonstrated successful reduction of the ileocecal intussusception [Fig. 3]. With alleviation of the patient's symptoms, he was discharged home. However, less than two days later, the symptoms recurred and he was admitted for further evaluation. Repeat abdominal ultrasound using a GE M12L transducer with pediatric abdomen settings at 8 MHz frequency demonstrated recurrent intussusception [Fig. 4]. Immediate exploratory laparotomy was performed without further studies, owing to suspicion of a pathologic lead point. At surgical exploration, an irreducible intussusception was found with wrinkling and indentation, or puckering, of the ileal serosa. Ileocecectomy was performed, and the patient made an unremarkable recovery.

The resected specimen consisted of a 9.5 cm segment of ileum and cecum with appendix. Encompassing about 75% of the ileocecal valve circumference was a 4.0 x 3.5 x 2.2 cm pale tan to pink fleshy tumor, covered by slightly hemorrhagic mucosa, extending through the ileal wall to the subserosal fat [Fig. 5]. Peri-ileal lymph nodes were palpable, but soft. Histologically, the tumor was a high grade lymphoma [Fig. 6], consisting of relatively monomorphic cells of intermediate size

with scant cytoplasm and 2-3 nucleoli. The cells molded to each other in a "mosaic tile" pattern. "Starry sky" pattern was prominent, with abundant mitoses. The cells stained positive for CD20, CD79a and CD10 immunohistochemical stains, confirming B-cells. Bcl-6 stain was positive. CD99 was negative. Ki-67 stain (cell proliferation marker) was positive in over 95% of the tumor cells. This morphology and immunohistochemical reactivity was consistent with Burkitt lymphoma, which was confirmed with fluorescent in situ hybridization (FISH), showing the IGH/MYC translocation [t(8;14)(q24;q32)]. Four slightly enlarged peri-ileal lymph nodes were found in the main specimen, and four regional lymph nodes, palpable at surgery, were sent separately to pathology. All nodes showed mild reactive changes and no evidence of lymphoma by histology and flow cytometry.

With the diagnosis of completely resected stage II Burkitt lymphoma, the patient received two cycles of multiagent chemotherapy, consisting of Cyclophosphamide, Vincristine, and Methotrexate. He remained without evidence of disease at eight months of follow up.

Case 2

A 16-year old Hispanic male presented with a history of painless, bright red blood-streaked stools for several weeks, followed by two days of abdominal pain, fever, and vomiting. Upon presentation to our Emergency Department, an acute abdomen series was obtained, which was nonspecific [Fig. 7]. A CT of the abdomen/pelvis with intravenous and oral contrast was then obtained utilizing a Phillips Brilliance 64 slice CT scanner at 78 mA and 120 kV with 3 mm slice thickness. CT demonstrated a large 8 cm mass in the pelvis with low attenuation and gas centrally, concerning for necrotic tumor and/or abscess/ulceration [Fig. 8]. Six hours later, delayed scans through the pelvis were performed on the same CT scanner at 99 mA and 120 kV with 3 mm slice thickness. This delayed scan helped to delineate the intraluminal extension and invasion of the mass into the small bowel [Fig. 9].

Laboratory values showed an elevated LDH level of 330 IU/L (normal, 98-192). At laparotomy, there was an 8 cm mass on the mesenteric aspect of the distal ileum that was involved with the lumen of the distal ileum causing partial obstruction with proximal dilated bowel. Peritoneal washings were performed, followed by an ileocecectomy with gross total removal of the mass. Some mildly enlarged ileocolic lymph nodes were sampled and a side to side functional end to end stapled anastomosis was created.

The resected specimen consisted of a 10.5 cm segment of terminal ileum, cecum (5 cm) and appendix. The terminal ileum showed a 9.2 x 7.4 x 6.5 cm exophytic grey-pink tumor, causing subtotal obstruction of the ileal lumen. Most of the tumor mass was located in the subserosa and the overlying serosa was hemorrhagic and focally disrupted [Fig. 10]. There was extensive hemorrhage within the tumor and central necrosis that extended to the mucosal surface and focally to the serosal surface of the tumor [Fig. 11]. Histologically, the tumor was a high grade lymphoma with morphologic, immunophenotypic, and molecular features of Burkitt lymphoma, similar to those described in Case 1. Twelve lymph nodes were found in the main specimen and three enlarged regional lymph nodes were sent separately. The nodes were mildly to moderately enlarged and soft. All showed benign reactive changes and no evidence of lymphoma by histology and flow cytometry. However, cytology from the peritoneal washings did reveal tumor cells.

On postoperative day 3, a Tc99m MDP whole body bone scan was performed on a Picker Prism 2000 Dual Head Nuclear Gamma Camera with medium energy collimator and 3-hour delayed imaging to evaluate for osseous metastasis. The examination was negative [Fig 12]. The patient also received a gallium scan on the same gamma camera with whole body, spot, and SPECT imaging with delayed scans performed at 72, 120, and 168 hours following 7 mCi Ga67 citrate intravenous injection. An intense focus of increased radiotracer uptake was identified in the left upper pelvis, possibly representing postsurgical, inflammatory changes but not exclusive of residual disease [Fig 13]. He was started on multiagent chemotherapy, consisting of Doxorubicin, Cyclophosphamide, Vincristine, and Methotrexate with adjuvant Mesna and Leucovorin. Nine months following his surgery and initiation of chemotherapy, the patient returned to our institution for follow up CT of the chest/abdomen/pelvis and a repeat gallium scan. Imaging performed on the Phillips Brilliance 64 slice CT scanner after administration of intravenous and oral contrast at 114 mA and 120 kV with 3 mm slice thickness demonstrated complete resolution of the pelvic mass [Fig. 14 a, b]. Furthermore, repeat gallium scan on the Prism 2000 gamma camera with delayed imaging at 120 and 168 hours following 7.7 mCi Ga67 citrate intravenous injection showed no abnormal radiotracer uptake [Fig. 14 c, d]. He remained free of disease at nine months follow up.

DISCUSSION

In the pediatric population, Burkitt lymphoma may present as an abdominal mass with symptoms such as gastrointestinal hemorrhage, abdominal pain, nausea, and intestinal obstruction caused by direct compression or involvement of the bowel lumen. In up to 18% of patients presenting with primary abdominal Burkitt lymphoma, intussusception is the presenting feature [1, 2]. We report two pediatric patients with Burkitt lymphoma of the ileocecal region, who presented in entirely different manners: one with recurrent intussusception, the other with gastrointestinal bleeding. In both cases, knowledge of the potential biology of Burkitt lymphoma, coupled with targeted radiologic workup and surgical therapy, contributed to favorable outcomes. Awareness of the multiple clinical presentations and imaging findings of Burkitt lymphoma is crucial for radiologists who treat children.

Non-Hodgkin lymphoma accounts for 40-50% of all lymphomas in children and adolescents. It represents approximately 6% of all malignancies in patients aged 0 to 19 [3]. Burkitt lymphoma comprises the large majority, though, of primary pediatric gastrointestinal tract lymphomas in the United States [4]. Compared to the United States, the

incidence of Burkitt lymphoma in Africa is approximately 50-fold higher, and this "endemic" form of Burkitt lymphoma typically presents as a jaw or facial bone tumor affecting younger children. It has been long suspected that this dramatically increased incidence is related to the prevalence of falciparum malaria in Africa and its association with Epstein-Barr virus (EBV) [5]. Burkitt lymphoma is a highly aggressive non-Hodgkin B-cell lymphoma that often presents at extranodal sites. It has a characteristic translocation involving the c-myc gene at band q24 on chromosome 8 [6].

Imaging features of gastrointestinal malignancy, including Burkitt lymphoma, have been described with GI fluoroscopy in the literature for several decades [7]. Sonography has also been used to evaluate extent of disease in the pediatric population [8]. However, CT is now frequently utilized as the initial imaging modality for patients with abdominal symptoms such as pain and gastrointestinal bleeding. Suggestion of intestinal lymphoma on CT plays an important role in the clinical management of patients with extra-nodal abdominal Burkitt lymphoma. Balthazar et al described two main patterns of small bowel lymphoma on CT, including symmetric or slightly asymmetric circumferential wall thickening and the "aneurysmal dilatation sign" [9]. The first pattern is seen with Case 1, in which the circumferentially thickened terminal ileum is seen intussuscepted into the cecum. The second pattern is demonstrated in Case 2, where dilatation of the terminal ileal lumen is seen with surrounding annular tumor encasement. Furthermore, Case 2 demonstrates central hypoattenuation and gas, compatible with necrosis/ulceration. Although these patterns are not specific for Burkitt lymphoma, raising the possibility of intestinal lymphoma in the differential can facilitate emergency department disposition of the patient and help guide clinical management.

In addition to CT, other modalities are available in the imaging of Burkitt lymphoma. Nuclear medicine imaging has been utilized for staging and monitoring, as was performed at our institution in Case 2. Gallium67 scintigraphy has been shown to detect all sites of tumor deposit, even those not detected by radiography, sonography, or CT [10]. As in our case, a whole body bone scan is frequently performed in conjunction with the gallium scan to evaluate for osseous metastasis. PET/CT has also been used to follow up and monitor treatment response for abdominal Burkitt lymphoma, although low positive predictive values and high false positive values have been reported [11]. MR enterography is a new modality that is being utilized for characterization of small bowel lymphoma. A study by Lohan et al described similar imaging features seen on CT, such as circumferential wall thickening, fold thickening, and loop dilatation, with the added MR benefits of lack of ionizing radiation, improved contrast and temporal resolution, and ability to image without administration of potentially nephrotoxic contrast agents [12].

Utilization of these various imaging modalities helps narrow the differential diagnosis in pediatric patients presenting with abdominal masses. Unfortunately, other forms of Non-Hodgkin lymphoma, including lymphoblastic lymphoma, blastic mantle cell lymphoma, and diffuse large B-cell lymphoma can exhibit similar imaging characteristics and thus mimic Burkitt lymphoma. Differentiation, of course, requires careful histopathologic analysis. In addition to lymphomas, other common pediatric intra-abdominal malignancies such as neuroblastoma and Wilms tumor must be excluded. Neuroblastoma is characterized on CT, MRI, and ultrasound as a heterogeneous, often invasive, mass arising from neuroblasts and occurring in sympathetic ganglia and adrenal medulla. Neuroblastoma is often further characterized by MIBG scan and Tc99m MDP bone scan for detection of osseous metastasis. Wilms tumor is a large heterogeneous mass arising from the kidney, which may or may not demonstrate local invasion and adenopathy. Knowledge of these imaging features can help focus the differential between retroperitoneal and intraperitoneal/intestinal lesions and guide the clinician to obtain surgical biopsy if intestinal lymphoma is suspected.

The utility of early tumor resection in children with extensive intra-abdominal Burkitt lymphoma, even in the setting of bowel obstruction, is not recommended. Surgical debulking of extensive disease may provoke tumor lysis syndrome, resulting in hyperuricemia and acute renal failure. Gahukamble et al found that the mortality after emergency laparotomy in the setting of untreated Burkitt lymphoma was very high and was not improved by aggressive tumor resection [13]. Furthermore, overly aggressive surgery may contribute to increased mortality [13, 14]. Patients with small tumors that are localized and can be safely resected may benefit from complete surgical resection. Except in rare instances in which a solitary lesion lends itself to total or near-total resection (i.e. at least 90% of the tumor can be resected), the proper role of surgery is a simple, safe procedure to obtain enough viable tumor for accurate diagnosis and prompt chemotherapy [15].

The two cases we report were resectable in straightforward fashion, rendering the patients free of disease without subjecting them to undue surgical stress or tumor lysis syndrome. In both cases, focused radiologic workup contributed to prompt surgical diagnosis and early initiation of chemotherapy. Physicians should remain aware of the myriad atypical presentations of pediatric Burkitt lymphoma arising in the gastrointestinal tract, and imaging studies in the pediatric patient should be directed with this in mind.

TEACHING POINT

Radiologists should be familiar with the myriad radiologic manifestations of pediatric gastrointestinal Burkitt lymphoma, including intussusception, intestinal wall thickening, and aneurysmal loop dilatation. Recognition of these imaging characteristics in the appropriate clinical setting leads to prompt diagnosis and favorable clinical outcomes.

REFERENCES

1. Gupta H, Davidoff AM, Pui CH, Shochat SJ, Sandlund JT. Clinical implications and surgical management of intussusception in pediatric patients with Burkitt lymphoma. J Pediatr Surg 2007;42(6):998-1001. PMID: 17560209.

2. Sorantin E, Lindbichler F. Management of intussusception. Eur Radiol 2004;14 Suppl 4:L146-154. PMID: 14752570.

3. Linabery AM, Ross JA. Childhood and adolescent cancer survival in the US by race and ethnicity for the diagnostic period 1975-1999. Cancer 2008;113:2575-2596. PMID: 18837040.

4. Kassira N, Pedroso FE, Cheung MC, Koniaris LG, Sola JE. Primary gastrointestinal tract lymphoma in the pediatric patient: review of 265 patients from the SEER registry. J Pediatr Surg 2011; 46:1956-1964. PMID: 22008334.

5. Ferry JA. Burkitt's lymphoma: clinicopathologic features and differential diagnosis. Oncologist 2006;11(4):375-383. PMID: 16614233.

6. Hecht JL, Aster JC. Molecular biology of Burkitt's lymphoma. J Clin Oncol 2000;18(21):3707-3721. PMID: 11054444.

7. Alford BA, Coccia PF, L'Heureux PR. Roentgenographic features of American Burkitt's lymphoma. Radiology. 1977 Sep;124(3):763-70. PMID: 887771.

8. Vade A, Blane CE. Imaging of Burkitt lymphoma in pediatric patients. Pediatr Radiol. 1985;15(2):123-6. PMID: 3883300.

9. Balthazar EJ, Noordhoorn M, Megibow AJ, Gordon RB. CT of small-bowel lymphoma in immunocompetent patients and patients with AIDS: comparison of findings. AJR Am J Roentgenol. 1997 Mar;168(3):675-80. PMID: 9057513.

10. Glass RB, Fernbach SK, Conway JJ, Shkolnik A. Gallium scintigraphy in American Burkitt lymphoma: accurate assessment of tumor load and prognosis. AJR Am J Roentgenol. 1985 Oct;145(4):671-6. PMID: 3898781.

11. Riad R, Omar W, Sidhom I, Zamzam M, Zaky I, Hafez M, Abdel-Dayem HM. False-positive F-18 FDG uptake in PET/CT studies in pediatric patients with abdominal Burkitt's lymphoma. Nucl Med Commun. 2010 Mar;31(3):232-8. PMID: 20032800.

12. Lohan DG, Alhajeri AN, Cronin CG, Roche CJ, Murphy JM. MR enterography of small-bowel lymphoma: potential for suggestion of histologic subtype and the presence of underlying celiac disease. AJR Am J Roentgenol. 2008 Feb;190(2):287-93. PMID: 18212211.

13. Gahukamble DB, Khamage AS. Limitations of surgery in intraabdominal Burkitt's lymphoma in children. J Pediatr Surg 1995;30(4):519-522. PMID: 7595824.

14. Abbasoglu L, Gun F, Salman FT, Celik A, Unuvar A, Gorgun O. The role of surgery in intraabdominal Burkitt's lymphoma in children. Eur J Pediatr Surg 2003;13(4):236-239. PMID: 13680491.

15. Stein JE, Schwenn MR, Jacir NN, Harris BH. Surgical restraint in Burkitt's lymphoma in children. J Pediatr Surg 1991;26(11):1273-1275. PMID: 1812254.

FIGURES

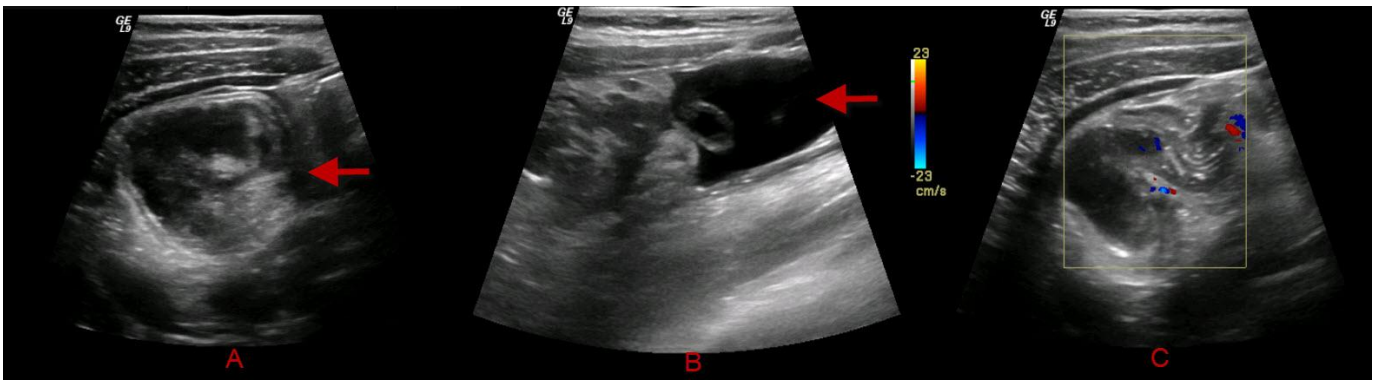

Figure 1: 7-year-old Caucasian male with ileal Burkitt lymphoma. Focused sonography of the right lower quadrant performed at initial presentation demonstrates a reniform-appearing mass in the right lower quadrant, suspicious for intussusception (arrow, A) with free fluid in the right lower quadrant (arrow, B). Minimal color flow is seen (C). (Protocol: GE M12L transducer with pediatric abdomen settings at 9 MHz frequency. Color flow images obtained at 5 MHz)

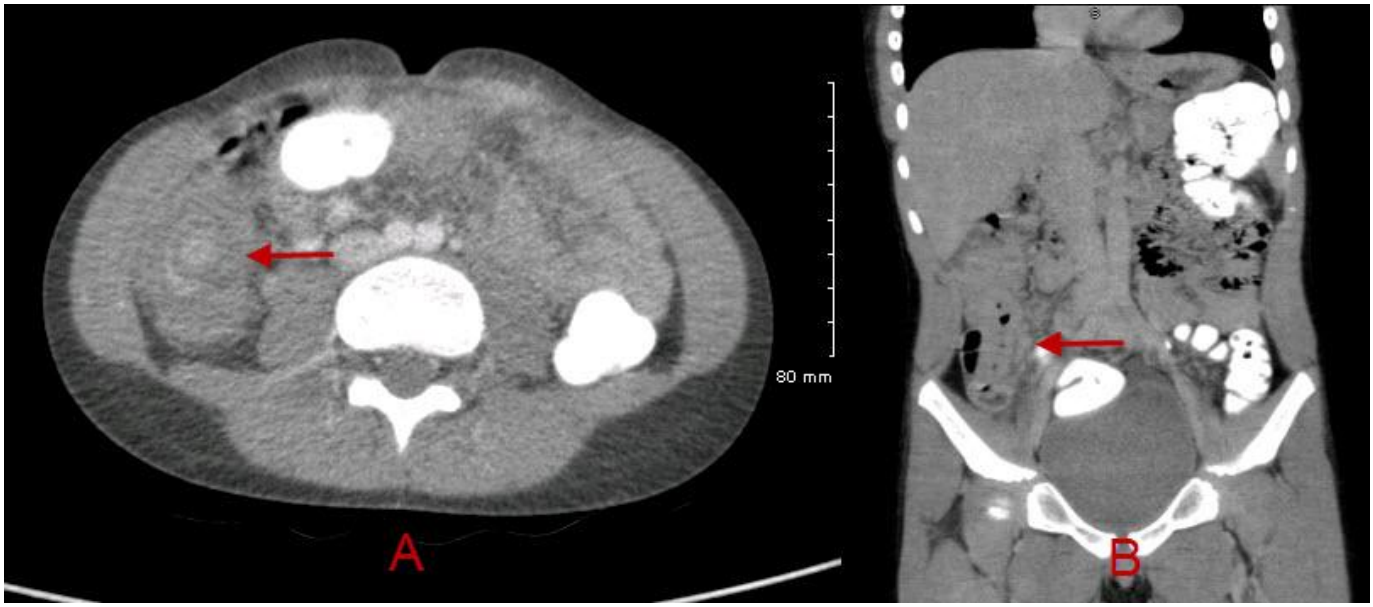

Figure 2: 7-year-old Caucasian male with ileal Burkitt lymphoma. Axial (A) and coronal (B) CT images of the abdomen and pelvis demonstrate a typical target-appearing lesion in the right lower quadrant, suggestive of intussusception of the terminal ileum into the cecum (arrows) with free fluid in the right paracolic gutter. (Protocol: Phillips Brilliance 64 slice CT scanner, 78 mA, 80 kV, 3 mm slice thickness, CTDIvol 0.842 mGy, 50 mL Optiray 350 IV contrast at 1 mL/s, 360 mL rectal contrast, no oral contrast)

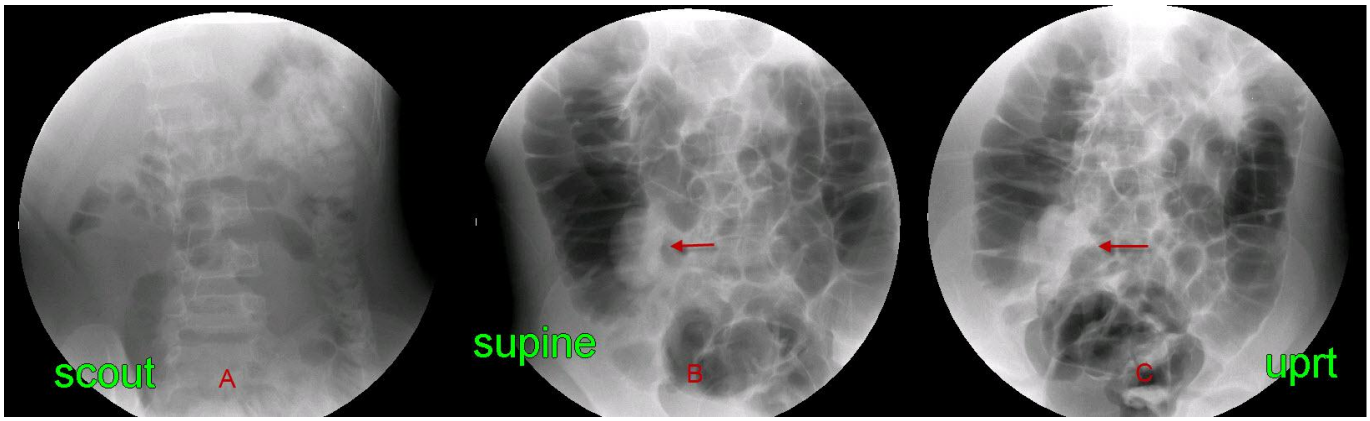

Figure 3: 7-year-old Caucasian male with ileal Burkitt lymphoma. Following initial diagnostic work-up, the patient was taken for air contrast enema. Scout (A), supine (B), and upright (C) views are provided. Residual oral contrast from the CT was seen in the transverse and descending colon. The ileocecal intussusception was successfully reduced by the radiologist. A lobulated wall-based soft tissue density at the ileocecal junction (arrows) was initially felt to represent an edematous ileocecal valve. In retrospect, this most likely represented the mass. (Protocol: Soft tip catheter placed intra-rectally and taped into position. Using fluoroscopic guidance, a sphygmometer was used with 120 mmHg pop off for maximum air pressure. Air was pumped into the colon for 5 minutes.)

Figure 4: 7-year-old Caucasian male with ileal Burkitt lymphoma. Focused sonography of the right lower quadrant demonstrates a "target sign," consistent with ileocecal intussusception (arrow). At this point, the patient was taken to the operating room for laparotomy with eventual ileocecectomy. (Protocol: GE 9L transducer with pediatric abdomen settings at 8 MHz frequency)

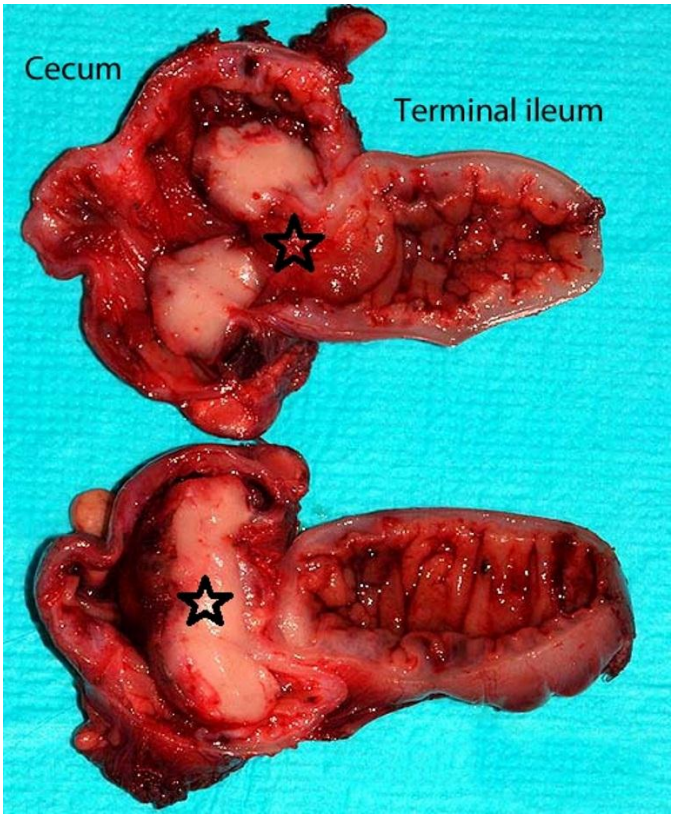

Figure 5: 7 year-old Caucasian male with ileal Burkitt lymphoma. Fleshy exophytic tumor (stars) involves most of the circumference of the ileocecal valve and bulges into the cecal lumen.

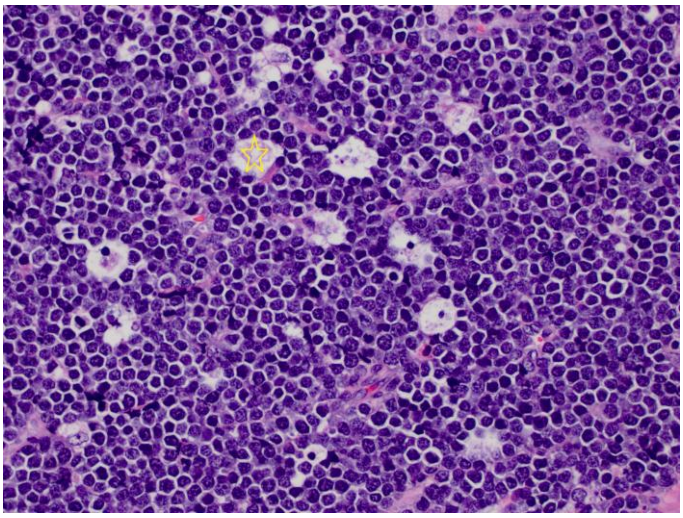

Figure 6: 7-year-old Caucasian male with ileal Burkitt lymphoma. The tumor is composed of monomorphic, intermediate size lymphocytes with "mosaic tile" molding of the cells, and "starry sky" pattern, with large tingible body macrophages containing cellular debris (star).

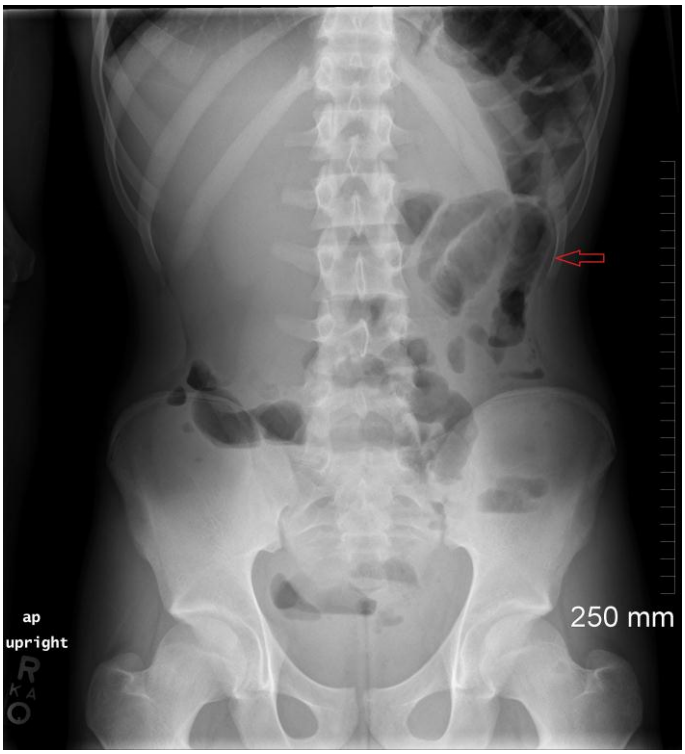

Figure 7: 16-year-old Hispanic male with ileal Burkitt lymphoma. Upright abdominal radiograph at initial presentation demonstrates a nonspecific bowel gas pattern with gaseous distention of several small bowel loops (arrow).

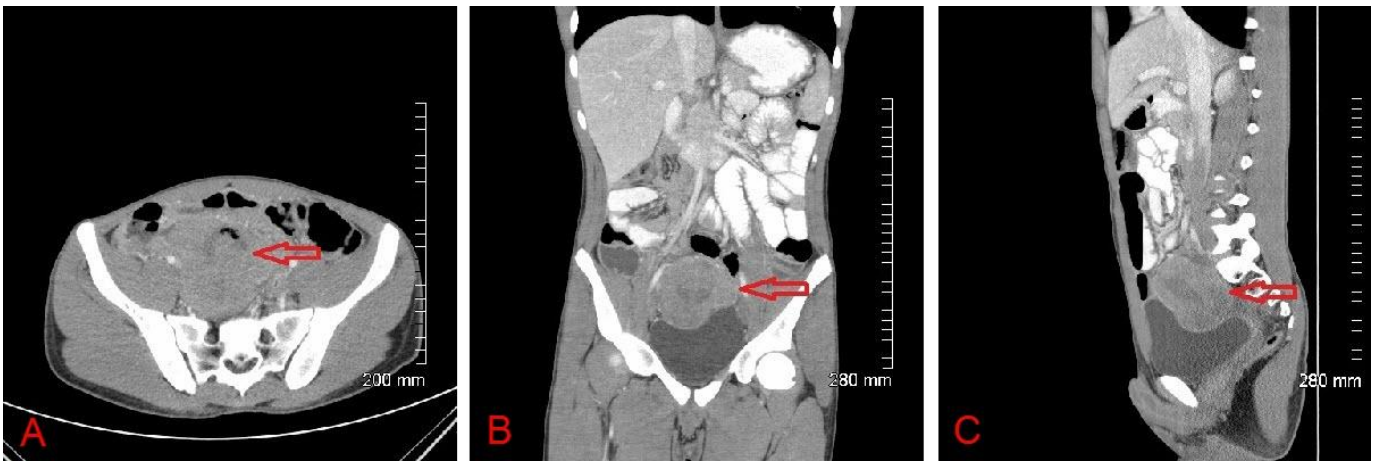

Figure 8: 16-year-old Hispanic male with ileal Burkitt lymphoma. Axial (A), coronal (B), and sagittal (C), contrasted CT of the abdomen/pelvis demonstrate an 8 cm mass at the level of the pelvic inlet with central hypoattenuation and gas, concerning for necrosis and abscess/ulceration (arrows). Further evaluation with delayed imaging was recommended. (Protocol: Phillips Brilliance 64 slice CT scanner, 78 mA, 120 kV, 3 mm slice thickness, CTDIvol 6.692 mGy, 110 mL Optiray 350 IV contrast at 2.5 mL/s, oral contrast)

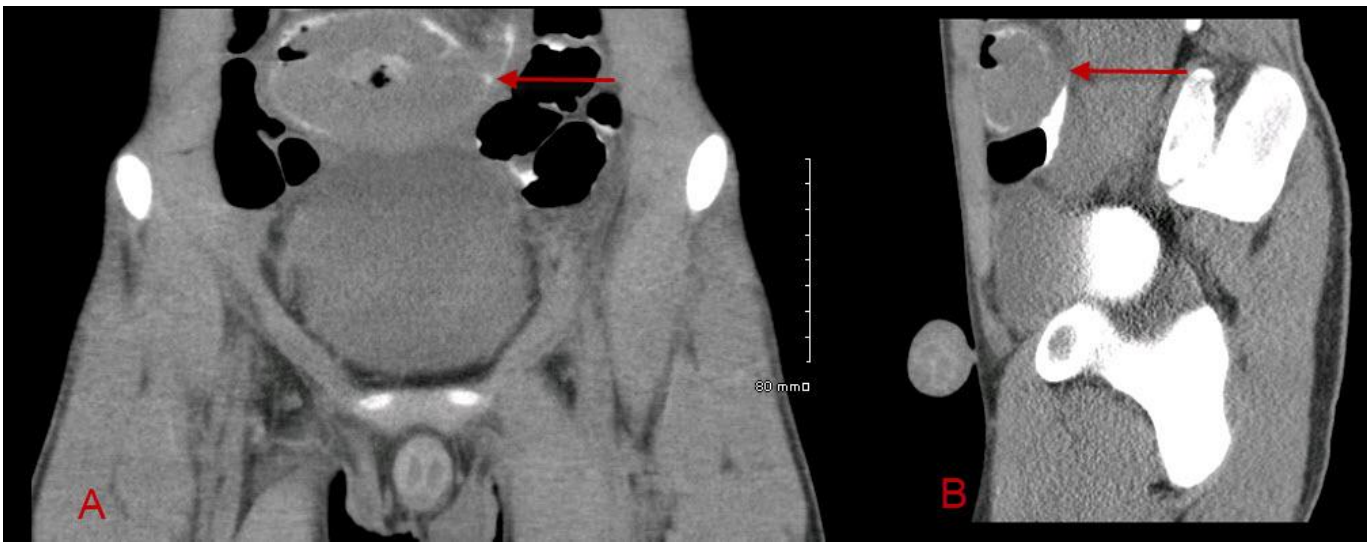

Figure 9: 16-year-old Hispanic male with ileal Burkitt lymphoma. Axial (A) and sagittal (B) delayed CT images were obtained through the pelvis six hours following the initial CT. This exam demonstrates the large pelvic mass outlined by oral contrast (arrows), suggesting intraluminal extension and invasion into the small bowel. The area of central necrosis is better delineated and correlates with pathology as described in Figure 11. (Protocol: Phillips Brilliance 64 slice scanner, 99 mA, 120 kV, 3 mm slice thickness, CTDIvol 4.875 mGy, 6 hour delay following original CT)

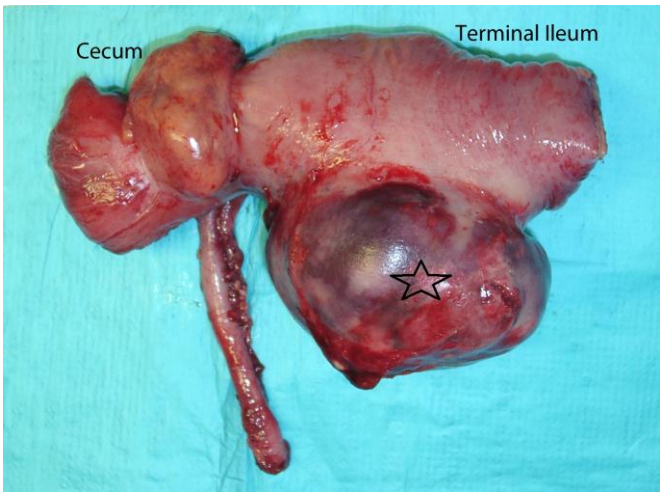

Figure 10 (left): 16-year-old Hispanic male with ileal Burkitt lymphoma. A large ileal tumor with overlying hemorrhagic serosa and focal disruption (star).

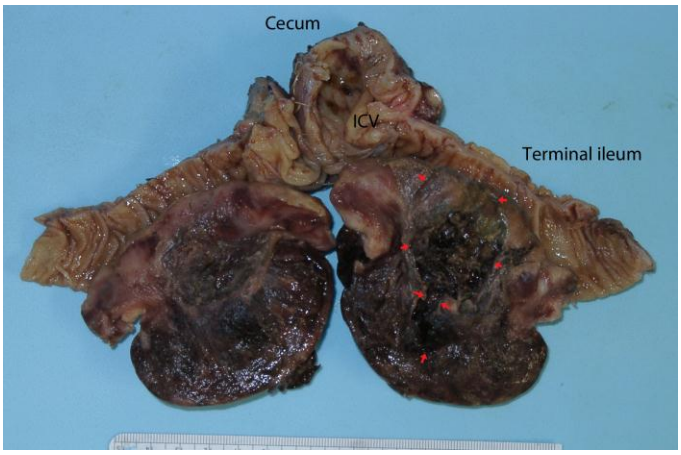

Figure 11: 16-year-old Hispanic male with ileal Burkitt lymphoma. Bisected specimen shows a fleshy tumor bulging into the ileal lumen, with extensive hemorrhage and central necrosis, outlined by the red arrows. Irregularity in the serosal surface is also demonstrated (on the left). The ileocecal valve (ICV) was not involved.

Figure 12: 16-year-old Hispanic male with ileal Burkitt lymphoma. Three days following surgery and pathologic diagnosis, the patient received a whole body bone scan to evaluate for osseous metastasis. Anterior and posterior views of the raw and truncated data are shown. No bony metastasis was identified. (Protocol: Picker Prism 2000 Dual Head Nuclear Gamma Camera with medium energy collimator, Radiotracer - 17.1 mCi Tc99m MDP intravenously, imaged 3 hours after administration)

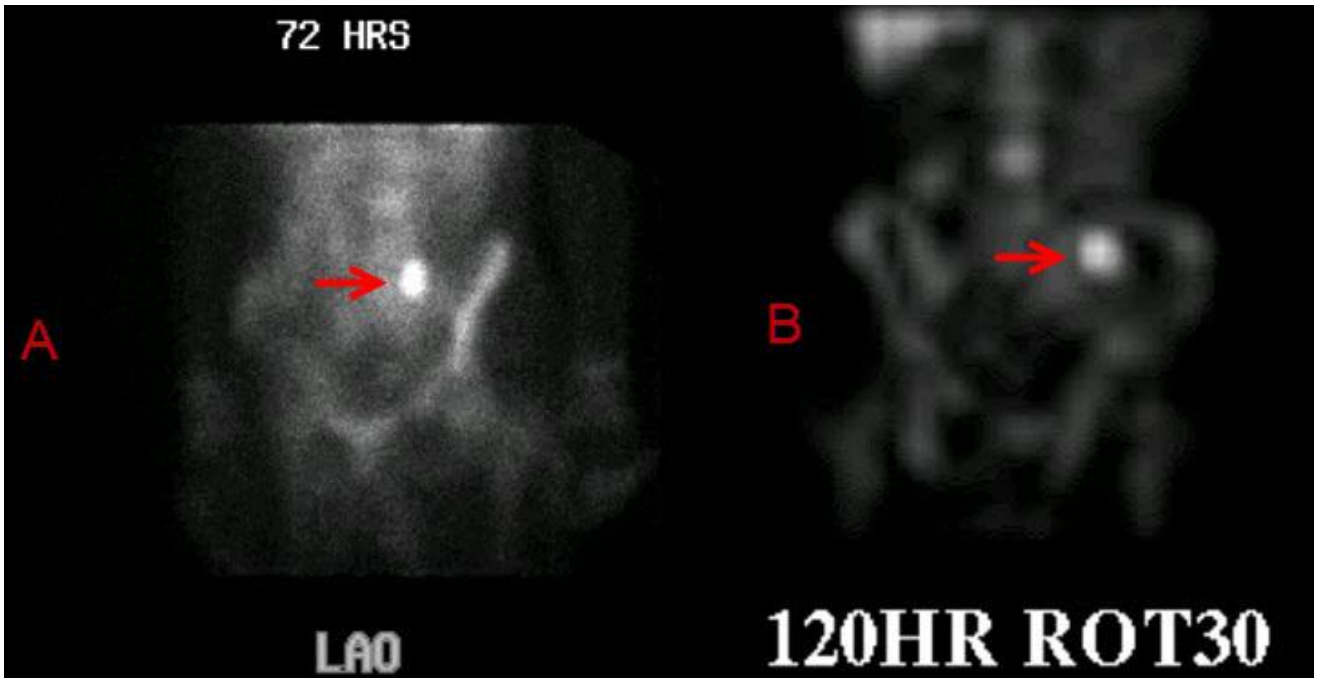

Figure 13: 16-year-old Hispanic male with ileal Burkitt lymphoma. Following whole body bone scan, the patient was imaged for a gallium scan to evaluate for residual tumor or extra deposits of Burkitt lymphoma not already identified. Images were obtained at 72, 120, and 168 hours following administration of Ga67 citrate. A spot LAO view at 72 hours and LAO SPECT image at 120 hours show intense activity in the left upper pelvis. It was thought that this may represent postsurgical, inflammatory changes but possibility of residual disease was considered given intense focal radiotracer uptake. (Protocol: Picker Prism 2000 Dual Head Nuclear Gamma Camera with medium energy collimator, 7 mCi Ga67 citrate via left chest Mediport; images obtained at 72, 120, and 168 hours following injection; Whole body, spot, and SPECT images were obtained)

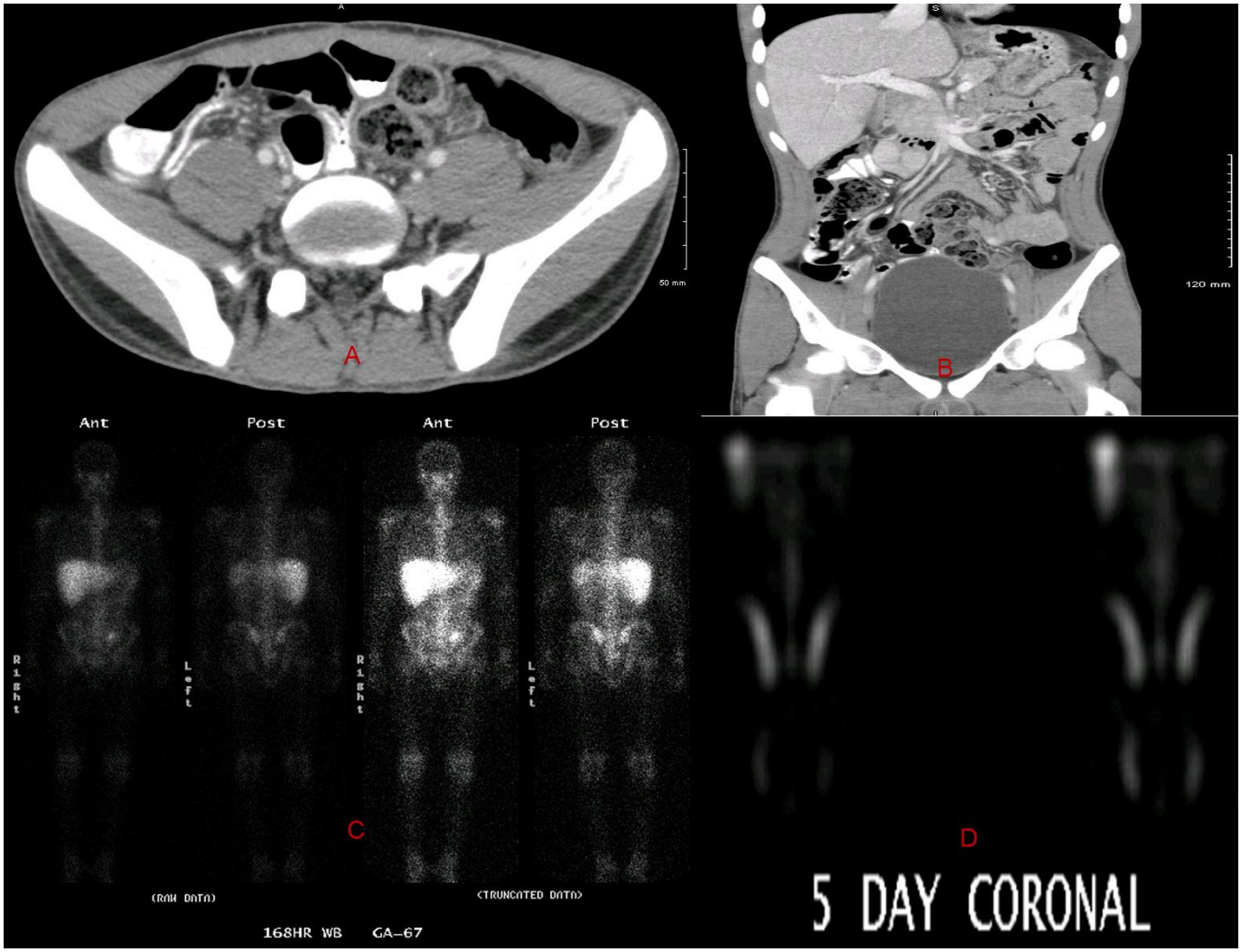

Figure 14: 16-year-old Hispanic male with ileal Burkitt lymphoma. Follow up CT and Ga67 scans were obtained after chemotherapy at a 9 month interval following surgical resection. Both studies demonstrated complete resolution of disease. Selected axial (A) and coronal (B) CT images of the abdomen/pelvis show complete resection of the mass without evidence of residual or recurrent disease. (Protocol: Phillips Brilliance 64 slice scanner, 114 mA, 120 kV, 3 mm slice thickness, CTDIvol 6.212 mGy, 100 mL Optiray 350 IV contrast, oral contrast). Selected anterior and posterior whole body gallium scan at 120 hours (C) and selected coronal SPECT images at 168 hours (D) show complete resolution of postsurgical increased radiotracer uptake. (Protocol: Picker Prism 2000 Dual Head Nuclear Gamma Camera with medium energy collimator, 7.7 mCi Ga67 citrate intravenously, imaged at 120 and 168 hours following radiotracer injection)

Etiology	• Highly aggressive non-Hodgkin B-cell lymphoma that often presents at extranodal sites
Incidence	• Comprises the large majority of primary pediatric gastrointestinal tract lymphomas in the United States • Estimated incidence ranges from one case per million for children less than ten years old, 0.7 per million from 10 to 20 and 0.6 per million from 20 to 30 • Rare in patients older than 30 • Incidence of gastrointestinal subtype of BL is not known
Gender Ratio	• 65-70% are male
Age Predilection	• 10-30 year old males
Risk Factors	• Link between Epstein Barr Virus (EBV) is not as strong in sporadic BL as with the endemic variety (African BL, involving jaw)
Presentation	• Abdominal pain, tenderness, intestinal obstruction, mass or intussusception • Fever is unusual • Rectal bleeding occurs in several patients with intussusception
Treatment	• Surgical resection and chemotherapy • Considered among the most responsive to chemotherapy
Prognosis	• Most authors have found that surgically resected patients with subsequent chemotherapy have a slightly higher survival rate • Nearly 80% of those with localized disease and more than half the children with more widespread disease are cured • Late relapses are hardly seen.
Differential	• Includes other tumors that present as abdominal masses and other types of NHL • In children, Wilms tumor and neuroblastoma are the most common intra-abdominal tumors • Others include different forms of lymphoma, leukemias with extensive extramedullary involvement, hepatic tumors, ovarian tumors, and soft tissue sarcomas • Among the other types of non-Hodgkin lymphoma, the most likely to be difficult to differentiate from Burkitt lymphoma are lymphoblastic lymphoma, blastic mantle cell lymphoma (which mimics the appearance of lymphoblastic lymphoma) and diffuse large B-cell lymphoma
Pathologic features	• Characteristic translocation involving the c-*myc* gene at band q24 on chromosome 8 • Over 80% of Burkitt lymphoma cases carry the t(8;14)(q24:q32) translocation • About 5-15% carry a t(2;8)(p12;q24) translocation, and about 5% have a t(8;22)(q24;q11) translocation
Imaging findings	• Children with non-endemic Burkitt lymphoma, the most common type seen in the United States, typically present with an abdominal mass • Abdominal x-rays can show a bowel gas pattern consistent with small bowel obstruction • Barium enema can be normal or demonstrate an intussusception (in the minority of patients) • In some patients, fluoroscopy shows a "string sign" in the terminal ileum, consistent with inflammatory bowel disease or tumor • Abdominal ultrasound can show a mass in the right lower quadrant warranting further workup for intussusception • Abdominal CT and MR enterography can show circumferential bowel wall thickening, nodular fold thickening, aneurysmal dilatation of the lumen, or a frank mass • Increased Ga^{67} uptake is seen with gallium scintigraphy • Increased FDG uptake can be seen in PET imaging • Osseous metastasis can be identified with Tc99m MDP bone scan

Table 1: Summary table for abdominal Burkitt lymphoma

Diagnosis	General Features	CT	MRI	US	Fluoro	NM
Burkitt and Burkitt-like lymphomas	• Can present as wall thickening or bulky, rapidly growing masses	• Circumferential symmetric or asymmetric bowel wall thickening • Dilated lumen vs. stricture • Focal mass • Bowel obstruction	• Circumferential wall thickening • Nodular fold thickening • Focal mass • Bowel obstruction	• "Doughnut sign" or "target sign" of intussusception • "Pseudokidney sign" with or without intussusception	• Ileocolic intussusception on air contrast enema, • "string sign"	• Increased Ga^{67} uptake on gallium scan • Increased FDG uptake on PET • Increased Tc99m MDP uptake in bones with osseous mets
Diffuse large B-cell lymphoma	• Can also present as bowel wall thickening • Sometimes large mass lesions, often localized	• Circumferential bulky intestinal wall mass, which may invade adjacent mesentery and lymphatics. Tumor may ulcerate and/or perforate.	• Intestinal wall mass, which may invade adjacent mesentery and lymphatics	• Hypoechoic mass with circumferential wall thickening	• Barium study: Polypoid, nodular, or ulcerative changes	• May also see increased Ga^{67} uptake on gallium scan and increased FDG uptake on PET
Neuroblastoma	• Embryonal malignancy of the sympathetic nervous system • Location: sympathetic ganglia, adrenal medulla, and other sites • Approximately 60% have abdominal primaries presenting as asymptomatic abdominal mass	• Heterogeneous mass from hemorrhage and/or necrosis • Invades vessels • May see calcification	• Heterogeneous, typically hypointense on T1 and hyperintense on T2 • Can evaluate for invasion into spinal canal	• Heterogeneous mass • Hypervascular on Color Doppler	• Not routinely utilized	• Frequently shows uptake of MIBG, related to catecholamine production • Can see calcified primary mass or bony metastasis on Tc99m MDP bone scan
Wilms Tumor	• Presents as asymptomatic abdominal mass with abdominal pain or hematuria occurring in 25% • WT-1 tumor suppressor mutation important in WAGR syndrome	• Large mass, replacing the kidney • Heterogeneous, poorly enhancing • Displaces adjacent organs • Can extend into perirenal fat and nearby lymph nodes, invade renal vein, IVC	• Heterogeneous, typically hypointense on T1 and hyperintense on T2	• Large, heterogeneous mass w or w/o local invasion and adenopathy • Color Doppler helpful to determine compression or invasion of venous structures	• Not routinely utilized	• May show increased FDG and Ga67 uptake • Tc99m MDP bone scan for osseous mets • Can use Tc99m DMSA to assess renal cortex function

Table 2: Differential diagnosis table for abdominal Burkitt lymphoma

ABBREVIATIONS

CT = Computed Tomography
EBV = Epstein-Barr virus
Ga = Gallium
GI = Gastrointestinal
MCi = milli Curie
MDP = Methylene Diphosphonate
MIBG = Metaiodobenzylguanidine
MR - Magnetic Resonance
MRI = Magnetic Resonance Imaging
PET = Positron Emission Tomography
SPECT = Single Photon Emission Computed Tomography
Tc = Technetium

KEYWORDS

Burkitt; lymphoma; gastrointestinal; pediatric